Electronic Supplementary Material (ESI) for Nanoscale.

Supporting information

Fully inkjet-printed transparent humidity sensor based on Ti_3C_2/Ag hybrid for touchless sensing of finger motion

Ning Li[‡], Yue Jiang[‡], Yan Xiao, Bo Meng, Chenyang Xing, Han Zhang[*] and Zhengchun Peng[*]

Key Laboratory of Optoelectronic Devices and Systems of Ministry of Education and Guangdong Province, College of Physics and Optoelectronic Engineering, Shenzhen University, Shenzhen 518060, China

[‡] These authors contributed equally to this work.

*To whom correspondence should be addressed. E-mail: hzhang@szu.edu.cn; zcpeng@szu.edu.cn

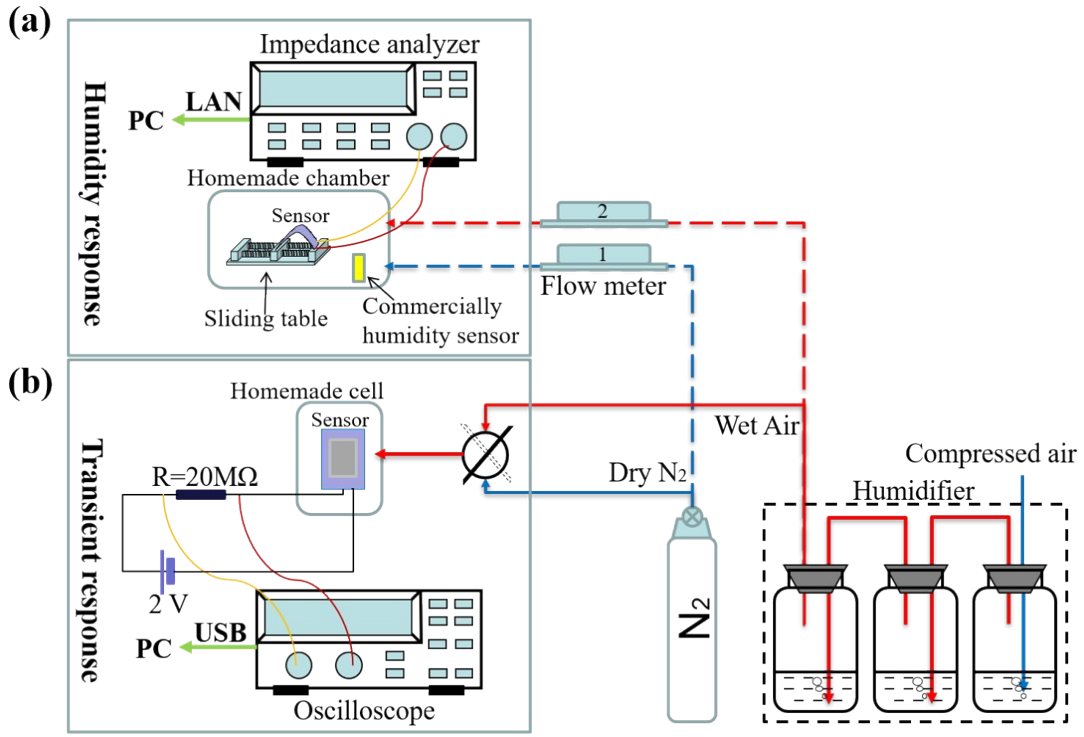

Fig. S1 A schematic diagram of the experimental setup. (a) The humidity sensing performance test system (Corresponding to the actual layout shown in Movie S1). (b) The transient response test system.

Movie S1 The actual layout of humidity sensing performance test system.

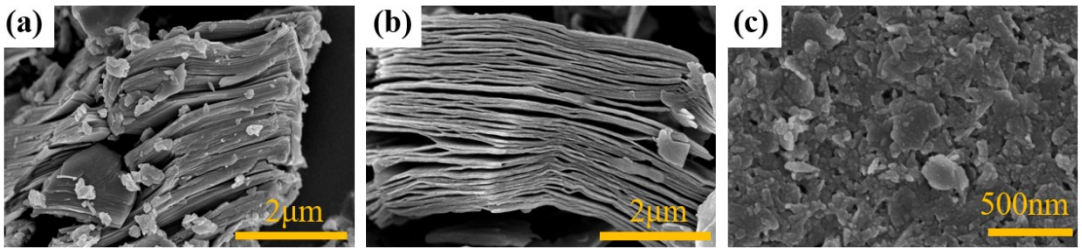

Fig. S2 SEM images of Ti_3AlC_2 (a), HF-etched Ti_3C_2 (b) and as-prepared 2D Ti_3C_2 MXene nanosheets (c).

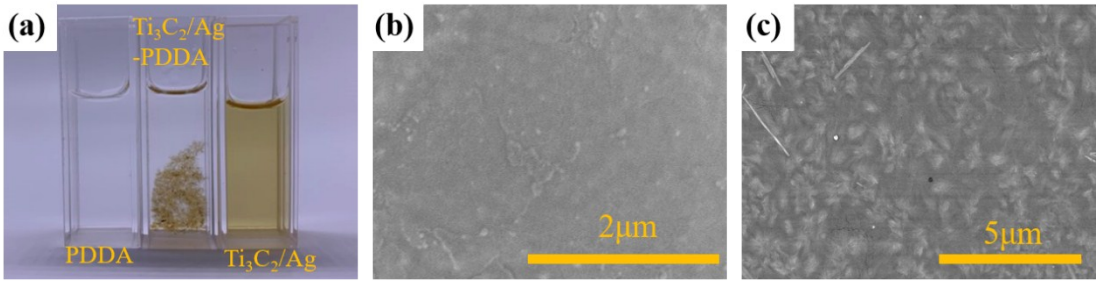

Fig. S3 (a) The physical drawing of PDDA, Ti_3C_2/Ag and Ti_3C_2/Ag-PDDA mixture. SEM images of pure PDDA films (b) and Ti_3C_2/Ag-PDDA bilayer (c) with no bending.

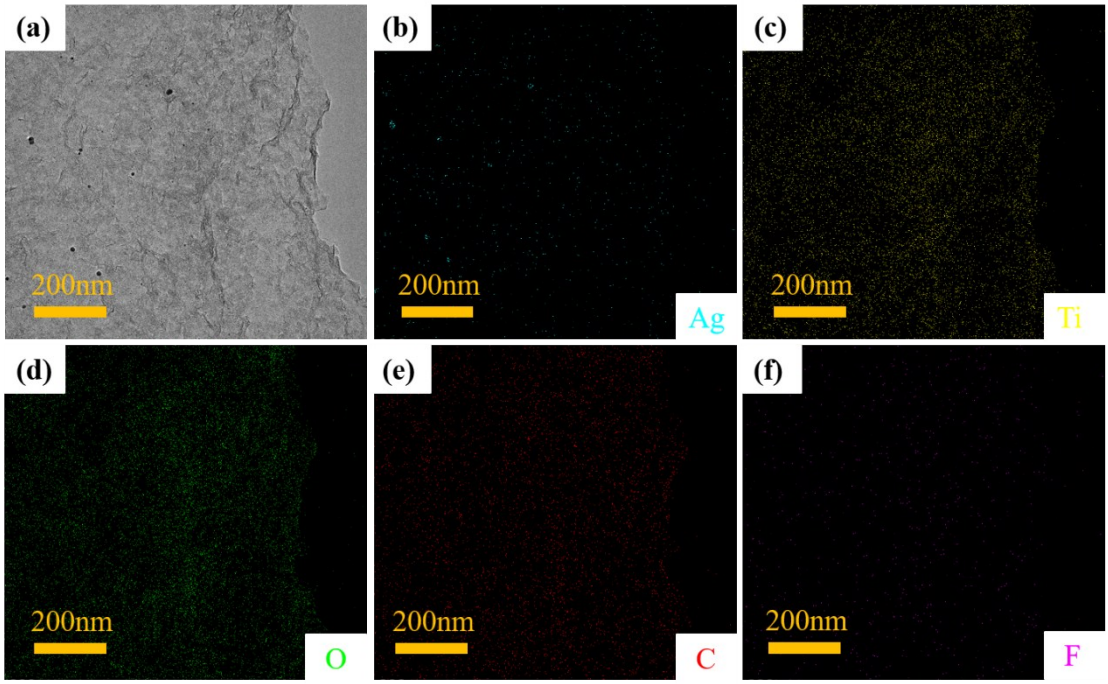

Fig. S4 **(a)** TEM image of Ti_3C_2/Ag hybrid. (b-f) EDS mapping of Ag, Ti, O, C and F.

Table S1 Atomic concentration and Mass concentration of elements on the surfaces of Ti_3C_2/Ag hybrid (Sample TA2) corresponding to Fig. S4.

Elements	*Ag*	*Ti*	*C*	*O*	*F*
Atomic Fraction (%)	0.32	14.91	29.92	53.82	1.03
Mass Fraction (%)	1.96	35.80	18.07	43.20	0.97

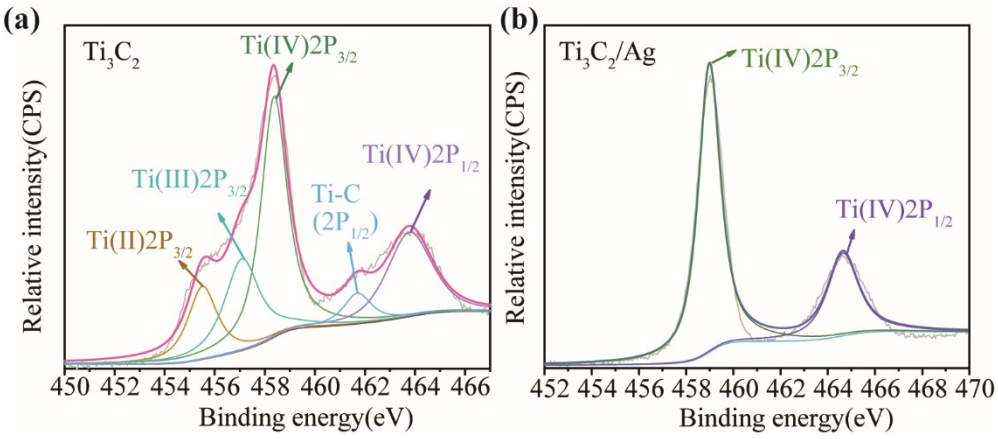

Fig. S5 X-ray photoelectron spectra (Ti 2p) of pure Ti_3C_2 (a) and Ti_3C_2/Ag hybrid (b), respectively.

Table S2 High performance humidity sensors reported in the literature.

Sensing materials	Sensing principe	Response time (s)	Recovery time (s)	Detection range (% RH)	Sensitivity (%)	References
GO	R	0.03	0.03	35-80	1000	34
MoS_2/SnO_2	C	5	13	0-97	3285000	36
MWCNT	R	2.5	3	30-90	10	38
Graphene/methyl-red	C	0.25	0.35	5-95	2869500	39
PEDOT:PSS/$ZnSnO_3$	R	0.2	0.2	0-90	2900	40
GDO	R	0.007	0.034	23-95	7500	41
Inkjet-printed graphene	R	7	55	10-80	17	42
Nafion	R	0.03	0.05	30-80	100	43
Silicon-nanocrystal	R	0.04	0.04	8-83	100000	44
Wrinkled Graphene	R	0.012	0.012	30-80	2.5	45
GNCP	R	0.02	0.017	0-97	28380	46
$Li_4Ti_5O_{12}$-TiO_2	R	9	17	11-95	1000	47
Li-doped GO	R	4	25	11-97	750	48
Li^+-doped SnO_2	R	1	1	10-90	500	49
MoS_2/ZnO QDs	Z	1	20	11-95	22000	50
N-Doped RGO Fiber	R	2	5	6-99	3.53	51
Pyranine/rGO	R	2	2	11-95	6000	52
PDI-4T	R	0.024	1	1-95	10000	53
SIM	R	0.037	0.09	11-86	23000	54
GO QDs	Z	1.5	1.5	7-97	181600	20
Ag-NA-rGO	Z	1	1	11-95	35000	55
Dopamine-melanin	R	0.42	0.43	0-100	10000	56
SnO_2/Fe	Z	1	3	10-95	647900	57
VO_2	R	0.5	0.5	30-95	10	58
CS-DMV	R	0.008	0.024	10-95	400	59
Ti_3C_2/Ag	C	0.08	0.12	10-95	106800	**This work**

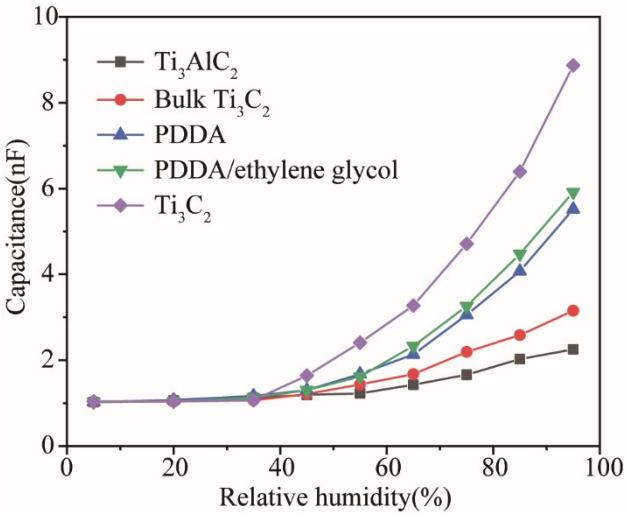

Fig. S6 Comparison of humidity sensitivity of sensors based on Ti_3AlC_2, HF-etched bulkTi_3C_2, pure Ti_3C_2, PDDA and PDDA/ ethylene glycol layers.

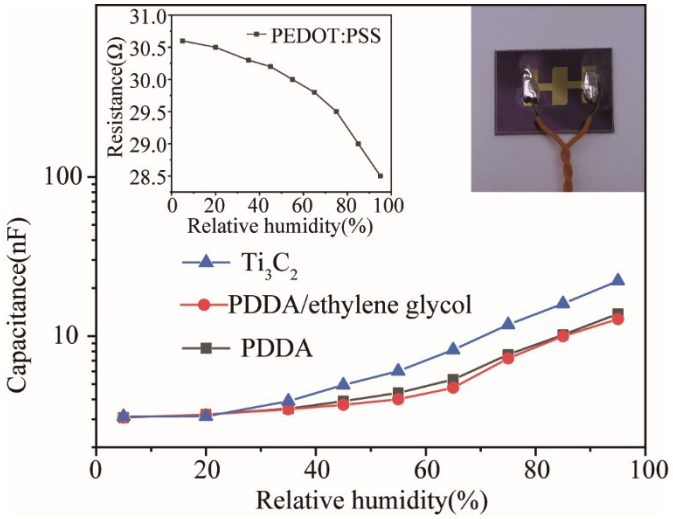

Fig. S7 Comparison of humidity sensitivity of sensors based on PEDOT: PSS, PDDA, PDDA/ ethylene glycol and pure Ti_3C_2 on the Au interdigital electrodes (silicon substrate).

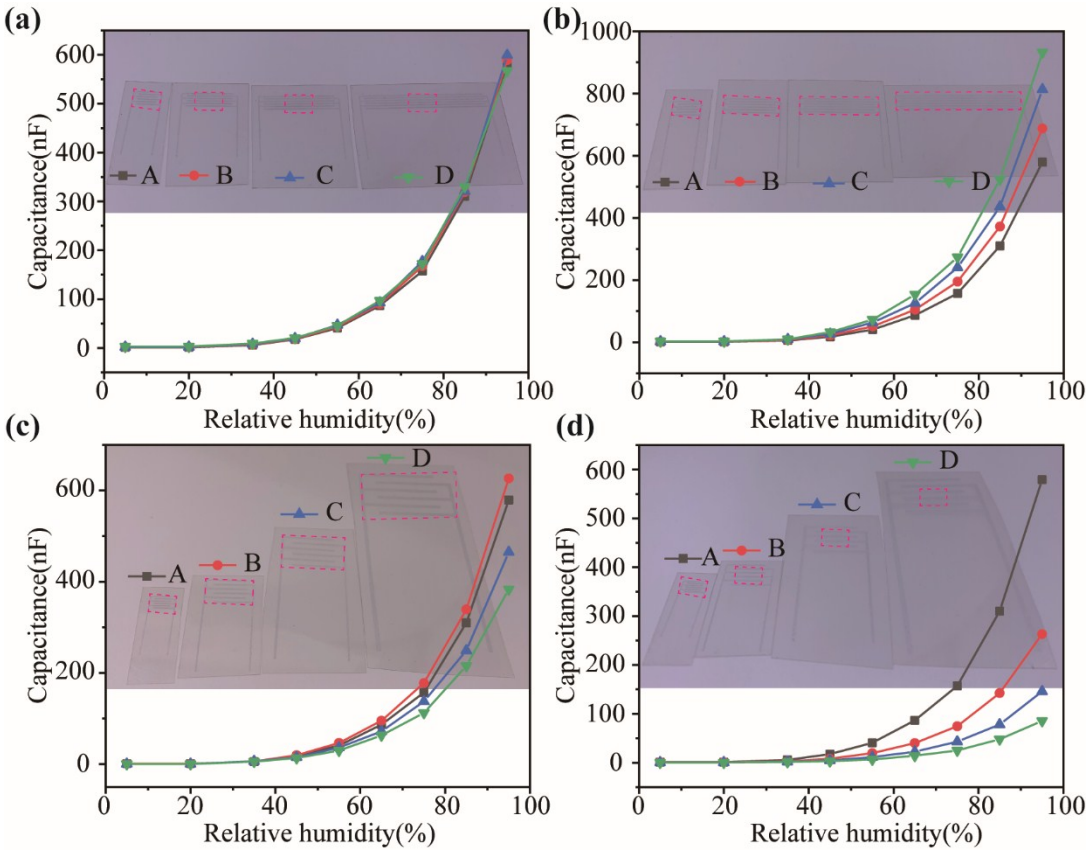

Fig. S8 Comparison of humidity sensitivity of sensors based on Ti_3C_2 with different length-width ratio of electrodes and different sizes of sensing layers.

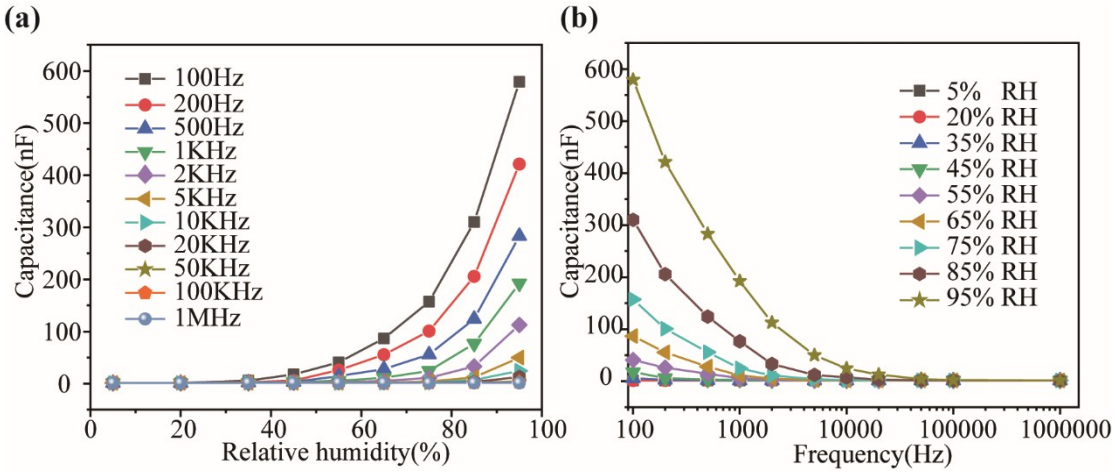

Fig. S9 (a) Capacitance versus RH for sensor TA2 under different operation frequency. (b) Capacitance versus the operation frequency for sensor TA2 at different humidity levels.

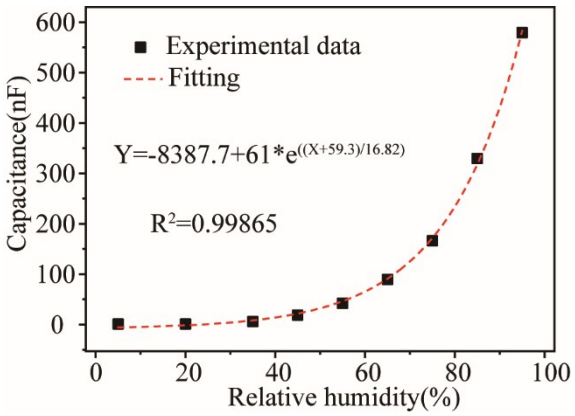

Fig. S10 Response of sensor TA2 as a function of RH.

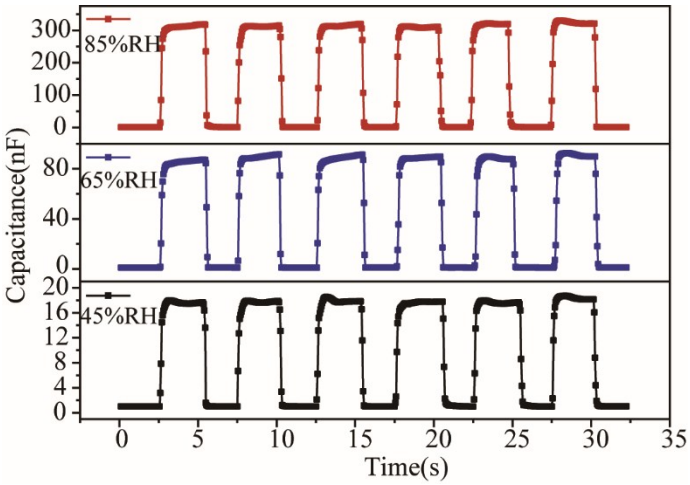

Fig. S11 Repeatability performance of sensor TA2 exposed to 45% RH, 65% RH, and 85% RH from dry N_2.

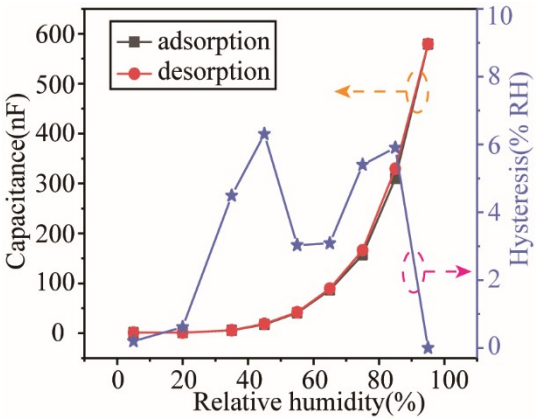

Fig. S12 Hysteresis curve of adsorption-desorption responses measured in the 5% - 95%RH range.

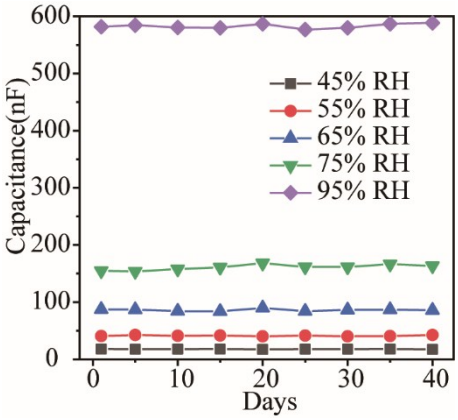

Fig. S13 Stable capacitance output of sensor TA2 under different humidity conditions for 40 days.

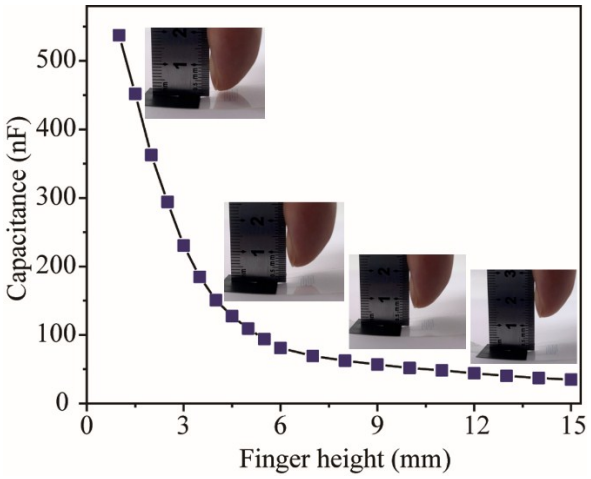

Fig. S14 Height-resolved capacitance diagram on the near surface of a fingertip measured by the as-established humidity sensor.

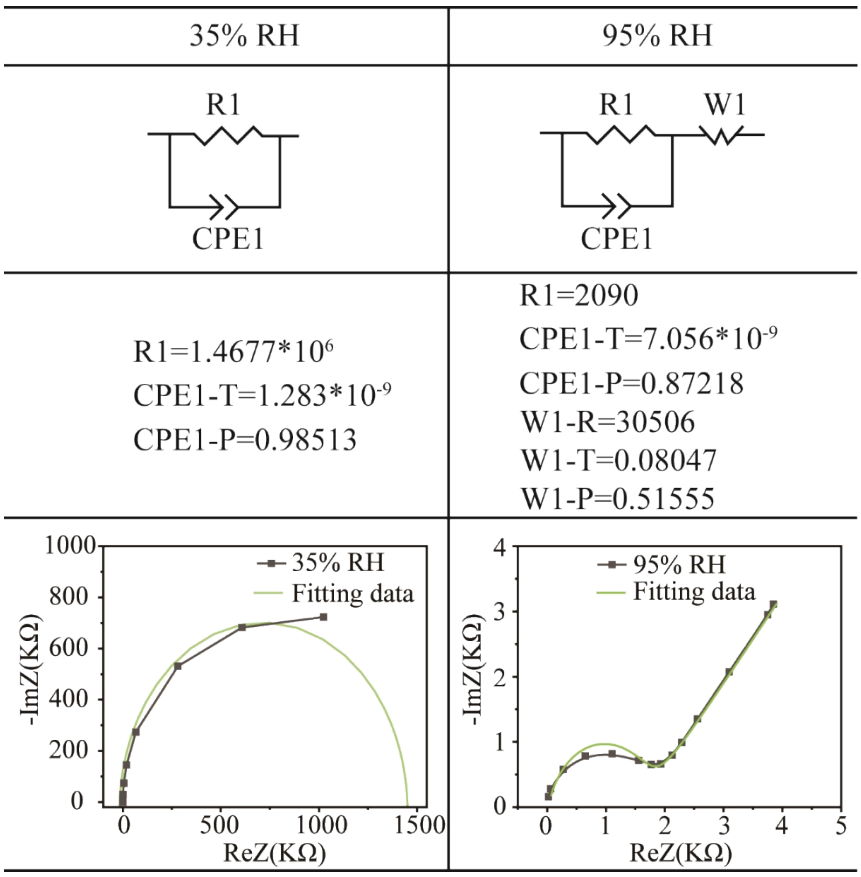

Fig. S15 Fitting result of the impedance spectra data by using the software Zview 3.3.

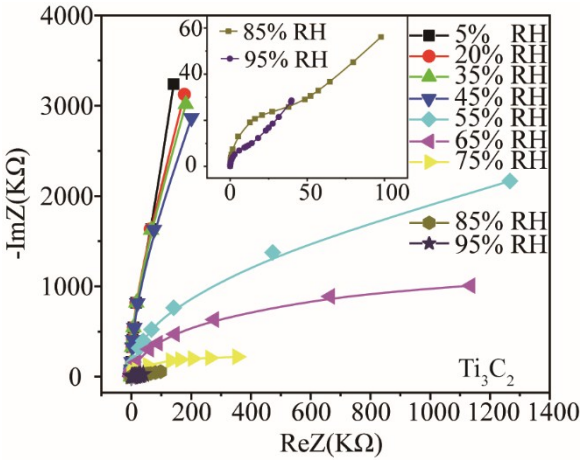

Fig. S16 Complex impedance plots of pure Ti_3C_2 film.

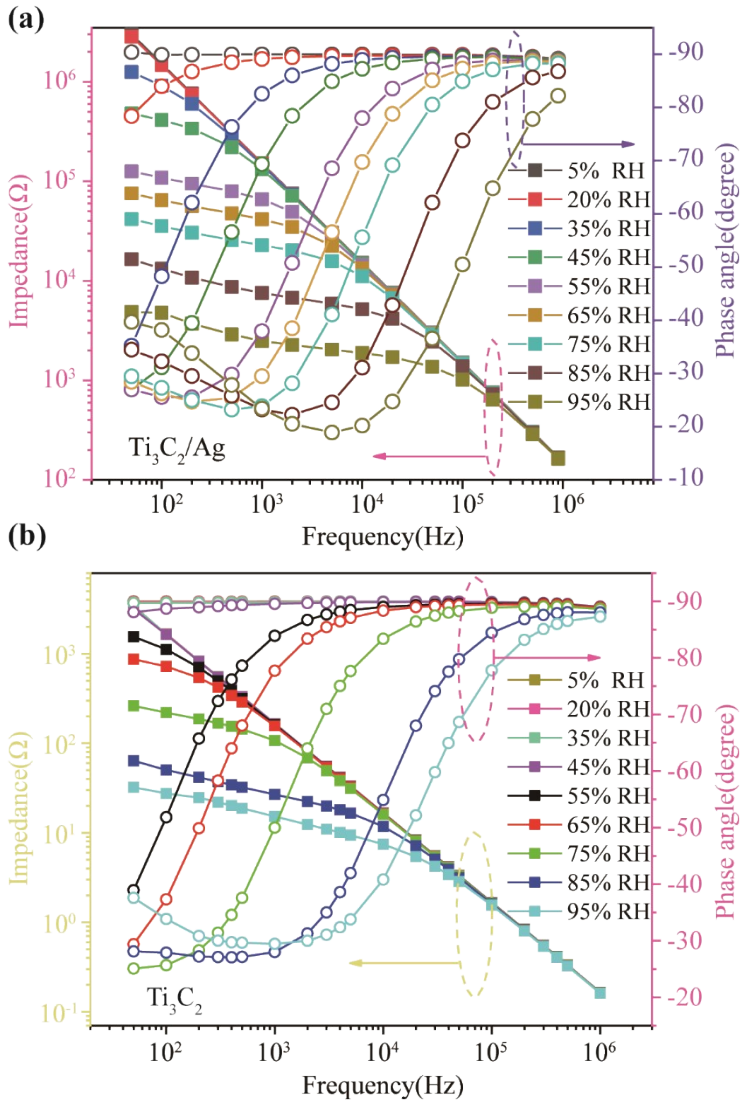

Fig. S17 Bode diagram of Ti_3C_2/Ag hybrid (a) and Ti_3C_2 (b).

Movie S2 The reconstructed dynamic information of the “knob turning motion” and “multiple fingers” state of human hands captured by the 3D noncontact positioning interface model.